Stable and conservative time propagators for second order hyperbolic systems

Kenneth Duru [*], Ken Mattsson [†], Gunilla Kreiss[‡]

April 5, 2011

Abstract

In this paper we construct a hierarchy of arbitrary high (even) order accurate explicit time propagators for semi-discrete second order hyperbolic systems. An accurate semi-discrete problem is obtained by approximating the corresponding spatial derivatives using high order accurate finite difference operators satisfying the summation by parts rule. In order to obtain a strictly stable semi-discrete problem, boundary conditions are imposed weakly using the simultaneous approximation term method. The time discretization starts with a second order central difference scheme, then using the modified equation approach (even in the presence of a first order derivative in time) we derive arbitrary high order accurate time marching schemes. For the fully discrete problem, we introduce a suitable weighted inner product and use the energy method to derive an optimal CFL condition, which provides a useful and rigorous criterion for stability. Numerical examples are also provided.

Keywords: Wave equations, hyperbolicity, higher order accuracy, discrete energy, stability, weighted inner product, ODE, SBP-SAT.

[*]Division of Scientific Computing, Department of Information Technology, Uppsala University Sweden

[†]Division of Scientific Computing, Department of Information Technology, Uppsala University Sweden and FOI, The Swedish Defence Research Agency, SE-164 90 Stockholm, Sweden

[‡]Division of Scientific Computing, Department of Information Technology, Uppsala University Sweden

1 Introduction

Numerical simulation of propagating waves is a challenge common to many branches of engineering and applied sciences. Relevant application areas are electromagnetics, acoustics, elasticity and general relativity. The equations modeling the phenomena of interest can often be written as a system of second order hyperbolic partial differential equations,

$$\mathbf{u}_{tt} = \mathcal{B}\mathbf{u}_t + \mathcal{D}\mathbf{u} + \mathbf{f}(\mathbf{x}, t), \quad \mathbf{x} \in \Omega \subset \mathbb{R}^d, \quad t > 0, \tag{1}$$

$$\mathcal{L}\mathbf{u} = \mathbf{g}, \quad \mathbf{x} \in \partial\Omega, \tag{2}$$

$$\mathbf{u} = \mathbf{u}_0, \quad \mathbf{u}_t = \mathbf{v}_0, \quad t = 0. \tag{3}$$

$\mathcal{D}$ is a self-adjoint[1] and negative definite spatial second order differential operator,

$$(\mathbf{u}, \mathcal{D}\mathbf{u}) = \left(\mathbf{u}, \mathcal{D}^\dagger \mathbf{u}\right) < 0, \quad \forall \mathbf{u} \neq 0.$$

$\mathcal{B}$ is also a spatial second order differential operator, and satisfies

$$\left(\mathbf{u}, \left(\mathcal{B} + \mathcal{B}^\dagger\right) \mathbf{u}\right) \leq 0.$$

$\mathcal{L}$ is a first order differential, boundary operator. The initial data, $\mathbf{u}_0$, $\mathbf{v}_0$, the source field, $\mathbf{f}(\mathbf{x}, t)$, and the boundary data, $\mathbf{g}$, are smooth functions which are compactly supported in Ω. $(\cdot, \cdot)$ denotes the standard $\mathrm{L}^2(\Omega)$ inner product,

$$(\mathbf{u}, \mathbf{v}) = \int_\Omega \mathbf{v}^* \mathbf{u} \mathrm{d}\mathbf{x},$$

where $\mathbf{v}^*$ is the conjugate transpose of $\mathbf{v}$. The unknown $\mathbf{u} : \Omega \times \mathbb{R}^+ \to \mathbb{C}^m$, is a bounded vector-valued function, the so-called wave function.

With homogeneous forcing and boundary data, and correct boundary operators $\mathcal{L}$, the system (1) – (3) has a bounded energy

$$\mathrm{E}_u(t) := (\mathbf{u}_t, \mathbf{u}_t) + (\mathbf{u}, -\mathcal{D}\mathbf{u}), \tag{4}$$

for all time.

In numerical treatment of (1) – (3), with few exceptions (for example [4, 6, 7, 11, 12]), the equations (1) – (3) are usually rewritten and solved as a first order system. This is in part due to the maturity of the theory and numerical techniques developed for CFD. While the theory and numerical methods for first order hyperbolic systems are well developed, numerical techniques to solve second order hyperbolic systems are less developed.

[1] $\mathcal{D}^\dagger$ denotes the adjoint operator.

In this paper we focus on time-stepping schemes for second order hyperbolic systems. We are particularly interested in high order accurate and efficient numerical simulations of time-dependent wave propagation problems, modeled by the time-dependent partial differential equations (PDE), (1) – (3). A popular approach to discretize time-dependent PDEs is the so called method of lines. That is, the full continuous problem is first reduced to a semi-discrete problem by first approximating all spatial derivatives. The method of lines technique applied to a second order wave equation, (1) – (3), leads to a system of second order ordinary differential equations (ODE) similar to (5). A fully discrete problem is then obtained by approximating the time derivatives with a suitable time propagator.

In the last decades a lot of effort has been devoted to high order accurate and stable spatial approximations of wave equations. For many problems, in the semi-discrete (discrete in space and continuous in time) setting, existing methods can accurately treat discontinuous coefficients, layered media, complex geometry, accurate and stable boundary procedures. In the finite difference time domain (FDTD), a stable and accurate spatial approximation of the standard wave equation can be derived using the SBP–SAT schemes (summation by parts operators (SBP) in combination with a weak boundary procedure, referred to as the simultaneous approximation term method (SAT)). In this case the semi-discrete problem has a bounded energy (is energy stable) for all time, see [6, 7, 4]. The SBP–SAT scheme (defined in Section 2) applied to the wave equations (1) – (3) yields,

$$\mathbf{v}_{tt} = B\mathbf{v}_t + D\mathbf{v} + \mathbf{F}(t), \quad t > 0, \quad \mathbf{v}(0) = \mathbf{u}_0, \quad \mathbf{v}_t(0) = \mathbf{v}_0. \tag{5}$$

In the system of ODEs (5), the coefficient matrices $B, D \in \mathbb{C}^{n\times n}$ are the corresponding discrete operators including weakly imposed boundary conditions. $\mathbf{F}(t)$ contains the forcing function $\mathbf{f}(\mathbf{x}, t)$ and the weakly imposed boundary data. The grid function $\mathbf{v} \in L^2$ is a bounded time dependent function, $\mathbf{v} : \mathbb{R}^+ \to \mathbb{C}^n$.

To retain a high order accurate and stable approximation in time one often rewrites (5) as a system of first order ODEs by introducing a new variable, $\mathbf{w} = \mathbf{v}_t$. Explicit Runge-Kutta schemes are then used to advance the solution in time. One drawback with this approach is that the number of unknowns is doubled (we also need additional memory to temporarily store the corresponding Runge-Kutta stages). The amount of work (CPU-time) needed to advance the solution one step in time can increase, by several orders. For Dirichlet boundary conditions, if there are no special treatment of the boundary conditions, this approach can lead to a dramatic loss of accuracy from the boundaries, see for instance [13, 14] and the references therein. We also note that the development of explicit local time-stepping schemes of arbitrarily high order accuracy based on Runge-Kutta schemes is a topic of active research while an explicit stability criterion still remains an open problem.

A potentially more efficient approach is to treat the ODE (5) in second order formulation. In the absence of a first order derivative in time, $B = 0$, it is easy to construct a two-step method, that is the second order 'Leap-Frog' scheme. This method was combined with a second and fourth order accurate finite difference approximations of the spatial derivatives for the scalar wave equation [12], and assuming that the matrix D is symmetric in L^2-scalar product, an energy technique was used to show stability. In [11] Gilbert and Joly considered a more general problem (5) also in the absence of a first order derivative in time, $B = 0$, and assuming $D^T = D$. Starting from the second order time-marching scheme Gilbert and Joly used the modified equation approach to construct a hierarchy of arbitrary high (even) order accurate methods. Using Fourier techniques and solving a non-convex optimization problem they could show that with increasing accuracy the CFL has an upper bound. Grote and Mitkova [3], Diaz and Grote [10] presented explicit local time stepping methods for Maxwell's equations when the spatial approximations are obtained with discontinuous Galerkin (DG) finite element discretization. In the absence of damping they derived a CFL condition which is bounded with increasing accuracy and showed that the numerical method conserves energy. In the presence of damping the scheme [3] is only second order accurate.

Here we consider semi-discrete problems resulting from high order accurate SBP-SAT schemes. If the semi-discrete problem is strictly stable, starting from a second order time-marching scheme we derive arbitrary high order accurate (and fully explicit) time-marching schemes. In a chosen weighted norm the fully discrete problem conserves energy in the absence of damping ($\Re B = 0$). In the presence of damping ($\Re B \leq 0$), the corresponding energy decays with time. The present technique is in spirit similar to [11, 12, 3, 10], but our approach is different since we can treat a more general class of problems. If the semi-discrete problem has a bounded energy, we can immediately derive arbitrary high order and stable approximation of the time derivatives. The analysis presented here is rooted in the construction of a discrete norm and a corresponding fully discrete energy that mimics the continuous and semi-discrete energies. By mimicking the continuous and semi-discrete energy estimates we show strict stability.

The outline of the paper is as follows. In Section 2, we introduce a model problem and derive the corresponding semi-discrete approximation. In Sections 3 and 4, we derive the schemes and prove stability. Numerical experiments are presented in Section 5. In Section 6 we offer a brief conclusion.

2 High order and stable semi-discrete approximation of the second order wave equation based on the SBP-SAT scheme

The focus of this paper is on time stepping schemes suitable for systems arising when applying the SBP-SAT technique to second order wave equations. We will in this section briefly review the SBP-SAT discretization of second order wave equations. More elaborate discussions can be found in [6, 7, 4].

We consider the damped scalar wave equation in one space dimension,

$$\begin{aligned} &u_{tt} = u_{xx} + \sigma(x)u_t + f(x,t), \quad x \in [a,b], \quad t > 0, \\ &u(x,0) = u_0(x), \quad u_t(x,0) = v_0(x), \quad \sigma(x) \le 0. \end{aligned} \tag{6}$$

$u_0(x)$, $v_0(x)$ and $f(x,t)$ are smooth functions which are compactly supported in $[a,b]$. In order to obtain a well-posed problem, we augment (6) with compatible boundary conditions,

$$\begin{aligned} \alpha_1 u_t + \beta_1 u_x + \gamma_1 u = g_1, \qquad x = a, \\ \alpha_2 u_t + \beta_2 u_x + \gamma_2 u = g_2, \qquad x = b. \end{aligned} \tag{7}$$

We will limit the study to those $\alpha_i, \beta_i, \gamma_i$ such that we have an energy estimate. Secondly, we shall always assume data to be sufficiently smooth, so that all derivatives needed in the analysis are well defined. To begin, we introduce the standard L_2-norm

$$\|u\|^2 = \int_\Omega u^* u \mathrm{d}\mathbf{x},$$

and the weighted norm

$$\|u\|_\rho^2 = \int_\Omega u^* \rho u \mathrm{d}\mathbf{x},$$

where $\rho(x) > 0$. We define the quantity

$$\mathrm{E}_u(t) := \|u_t\|^2 + \|u_x\|^2 - \frac{\gamma_1}{\beta_1} u^2|_a + \frac{\gamma_2}{\beta_2} u^2|_b. \tag{8}$$

The quantity $\mathrm{E}_u(t)$ is an energy if $\mathrm{E}_u(t) \geq 0$, $\forall t > 0$, and if $E_u(t) = 0$ implies that $u(x,t) = const$.

Lemma 1 *Consider the quantity* $\mathrm{E}_u(t)$ *defined by (8). If* $\beta_1 < 0$, $\beta_2 > 0$, $\gamma_i \geq 0$, *the quantity* $\mathrm{E}_u(t)$ *is an energy.*

Proof:

The conditions on β_i, γ_i imply $\mathrm{E}_u(t) \geq 0$. If $E_u(t) = 0$, then $u_t = 0$ and $u_x = 0$. If γ_1 or γ_2 is nonzero then $u = 0$. Therefore $\mathrm{E}_u(t) \geq 0$ is an energy. □

Theorem 1 *Consider the wave equation (6) with $\sigma_0 = \min_x \sigma(x) < 0$. Consider also the boundary conditions (7) with a general inhomogeneous data g_1, g_2. If the conditions in Lemma 1 hold, if in addition $\alpha_i \geq 0$, then the energy $\mathrm{E}_u(t)$ satisfies*

$$\mathrm{E}_u(t) \leq \mathrm{E}_u(0) + K \int_0^t \left(\|f(\tau)\|^2 + |g_1(\tau)|^2 + |g_2(\tau)|^2 \right) d\tau, \quad K > 0. \tag{9}$$

Proof:

To derive the estimate (9), we multiply (6) with u_t^* and add the conjugate transpose of the product. Integration by parts yields

$$\frac{d}{dt}\|u_t\|^2 = -\frac{d}{dt}\|u_x\|^2 + 2u_t u_x|_a^b - \|u_t\|^2_{|\sigma|} + (u_t, f) + (f, u_t). \tag{10}$$

We insert the boundary condition (7) and we have

$$\begin{aligned}\frac{d}{dt}\left(\|u_t\|^2 + \|u_x\|^2 - \frac{\gamma_1}{\beta_1}u^2|_a + \frac{\gamma_2}{\beta_2}u^2|_b \right) &= -\|u_t\|^2_{|\sigma|} + \frac{\alpha_1}{\beta_1}u_t^2|_a - \frac{\alpha_2}{\beta_2}u_t^2|_b + (u_t, f) \\ &+ (f, u_t) + \frac{\alpha_2}{\beta_2}g_2 u_t|_b - \frac{\alpha_1}{\beta_1}g_1 u_t|_a.\end{aligned} \tag{11}$$

We can identify the energy $\mathrm{E}_u(t)$ in (15).

If $\alpha_i \geq 0$, then

$$\begin{aligned}\frac{d}{dt}E_u(t) &\leq -\|u_t\|^2_{|\sigma|} + (f, u_t) + (u_t, f) + \frac{\alpha_2}{2\beta_2}|g_2|^2 + \frac{\alpha_1}{2|\beta_1|}|g_1|^2 \\ &\leq \frac{1}{\sigma_0}\|f(t)\|^2 + \frac{\alpha_2}{2\beta_2}|g_2|^2 + \frac{\alpha_1}{2|\beta_1|}|g_1|^2.\end{aligned}$$

Time-integration yields

$$E_u(t) \leq \mathrm{E}_u(0) + K \int_0^t \left(\|f(\tau)\|^2 + |g_1(\tau)|^2 + |g_2(\tau)|^2 \right) d\tau, \tag{12}$$

where $K > 0$ is a constant. □

Consider now homogeneous boundary data.

Theorem 2 *Consider the wave equation (6), subject to the boundary conditions (7) with homogeneous data $g_1 = 0$, $g_2 = 0$. If the conditions in Lemma 1 hold, if in addition $\alpha_i \geq 0$, then the energy $\mathrm{E}_u(t)$ satisfies*

$$\sqrt{\mathrm{E}_u(t)} \leq \sqrt{\mathrm{E}_u(0)} + K \int_0^t \|f(\tau)\| d\tau, \quad K > 0. \tag{13}$$

Proof:

As before, we multiply (6) with u_t^* and add the conjugate transpose of the product. Integration by parts yields

$$\frac{d}{dt}\|u_t\|^2 = -\frac{d}{dt}\|u_x\|^2 + 2u_t u_x|_a^b - \|u_t\|_{|\sigma|}^2 + (u_t, f) + (f, u_t). \tag{14}$$

We insert the boundary condition (7) and we have

$$\frac{d}{dt}\left(\|u_t\|^2 + \|u_x\|^2 - \frac{\gamma_1}{\beta_1}u^2|_a + \frac{\gamma_2}{\beta_2}u^2|_b\right) = -\|u_t\|_{|\sigma|}^2 + \frac{\alpha_1}{\beta_1}u_t^2|_a - \frac{\alpha_2}{\beta_2}u_t^2|_b + (u_t, f) + (f, u_t). \tag{15}$$

If $\alpha_i \geq 0$, then

$$\begin{aligned} \frac{d}{dt}E_u(t) &\leq -\|u_t\|_{|\sigma|}^2 + (f, u_t) + (u_t, f) \\ &\leq 2\|u_t\|\|f(t)\|. \end{aligned}$$

We write $E_u(t) = \sqrt{E_u(t)}\sqrt{E_u(t)}$. Using the fact $\sqrt{E_u(t)} \geq \|u_t\|$, yields

$$2\sqrt{E_u(t)}\frac{d}{dt}\sqrt{E_u(t)} \leq 2\sqrt{E_u(t)}\|f(t)\|.$$

If $E_u(t) > 0$, time-integration yields

$$\sqrt{E_u(t)} \leq \sqrt{\mathrm{E}_u(0)} + K \int_0^t \|f(\tau)\| d\tau, \tag{16}$$

where $K > 0$ is a constant. □

The following definition is central to the present study:

Definition 1 (Strict stability) *A discrete approximation of a time-dependent PDE is strictly stable, if for a fixed mesh-size $h > 0$, the corresponding discrete equation does not allow any growth not permitted by the PDE as time goes to infinity, $t \to \infty$.*

For time-dependent problems, strict stability is an important property, particularly if long-time calculations are desired. We note that for IBVPs, it is difficult to derive strictly stable and higher order accurate schemes. Our goal is to construct higher order accurate and strictly stable fully discrete approximations of the second order hyperbolic system (1), for some boundary conditions (2). To demonstrate our approach we consider the model problem (6) and the boundary conditions (7). By mimicking the energy estimate (13), we derive strictly stable semi-discrete and fully discrete approximations of (6). We will begin with the semi-discrete scheme in this section and proceed to the fully discrete approximation in the next section.

2.1 Semi-discrete approximation

If the conditions in Theorem 2 hold, we can rewrite the boundary conditions (7) as

$$\begin{aligned} \frac{\alpha_1}{|\beta_1|}u_t - u_x + \frac{\gamma_1}{|\beta_1|}u - \frac{g_1}{|\beta_1|} &= 0, \qquad x = a, \\ \frac{\alpha_2}{\beta_2}u_t + u_x + \frac{\gamma_2}{\beta_2}u - \frac{g_2}{\beta_2} &= 0, \qquad x = b. \end{aligned} \tag{17}$$

Discretising the spatial domain into N equidistant grid points, i.e.,

$$x_j = a + (j-1)h, \qquad j = 1, 2 \dots, N, \qquad h = \frac{b-a}{N-1}.$$

The numerical approximation of the solution at the grid point x_j is denoted $v_j(t)$ and the semi-discrete solution vector $\mathbf{v}(t) = [v_1(t), v_2(t), v_3(t), \dots, v_N(t)]^T$. The semi-discrete equivalent of the boundary conditions (7) or (17) is

$$B_s\mathbf{v}_t + B_n D_x\mathbf{v} + B_e\mathbf{v} - \mathbf{G}(t) = 0, \tag{18}$$

where

$$B_s = diag\left(\frac{\alpha_1}{|\beta_1|}, 0, 0, \dots, \frac{\alpha_2}{\beta_2}\right), \quad B_n = diag\left(-1, 0, 0, \dots, 1\right).$$

$$B_e = diag\left(\frac{\gamma_1}{|\beta_1|}, 0, 0, \dots, \frac{\gamma_2}{\beta_2}\right), \quad \mathbf{G}(t) = \left[\frac{g_1}{|\beta_1|}, 0, 0, \dots, 0, \frac{g_2}{\beta_2}\right]^T.$$

The operator D_x is a consistent finite difference approximation of the first derivative u_x on the boundaries. An SBP discretisation of (6) with a SAT implementation of the boundary conditions (17) reads

$$\begin{aligned} \mathbf{v}_{tt} =& D_{xx}\mathbf{v} + \Sigma\mathbf{v}_t - \tau_n H^{-1}\left(B_s\mathbf{v}_t + B_n D_x\mathbf{v} + B_e\mathbf{v} - \mathbf{G}(t)\right) + \tilde{\mathbf{f}}(\mathbf{x}, t), \\ & \mathbf{v}(0) = \mathbf{u}_0, \qquad \mathbf{v}_t(0) = \mathbf{v}_0. \end{aligned} \tag{19}$$

Here $\tilde{\mathbf{f}}(\mathbf{x},t)$ contains the grid values of the forcing $f(x,t)$, $\mathbf{G}(t)$ is the boundary data, and

$$\Sigma = diag(\sigma_1, \sigma_2, \dots, \sigma_N).$$

The operator D_{xx} is an SBP operator and satisfies

$$\begin{aligned} &D_{xx} = H^{-1}(-M + B_n D_x), \quad M = M^T, \quad \mathbf{v}^* M \mathbf{v} \geq 0, \quad \forall \mathbf{v} \neq 0, \\ &H = H^T, \quad \mathbf{v}^* H \mathbf{v} > 0, \quad \forall \mathbf{v} \neq 0, \end{aligned} \tag{20}$$

see [9]. In addition we assume that M has a simple zero eigenvalue corresponding to the eigenvector $\mathbf{v}_0 = const[1, 1, \cdots, 1]^T$. That is $\mathbf{v}^* M \mathbf{v}$ mimics $\|u_x\|^2$, which is zero only if u does not vary in space. This is true if D_{xx} corresponds to a narrow finite difference stencil. The penalty parameter, τ_n, is determined by stability. We can rewrite (19) as

$$\begin{aligned} &\mathbf{v}_{tt} = B\mathbf{v}_t + D\mathbf{v} + \mathbf{F}(t), \\ &\mathbf{v}(0) = \mathbf{u}_0, \qquad \mathbf{v}_t(0) = \mathbf{v}_0. \end{aligned} \tag{21}$$

Here

$$D = -H^{-1}A, \quad B = -H^{-1}C,$$

$$A = M - B_n D_x + \tau_n B_n D_x + \tau_n B_e, \quad C = \tau_n B_s - H\Sigma,$$

and

$$\mathbf{F}(t) = \tau_n H^{-1}\mathbf{G}(t) + \tilde{\mathbf{f}}(\mathbf{x},t).$$

We will show that the correct choice of the penalty parameter τ_n, leads to strict stability.

Definition 2 *Let C be a given complex matrix. C^* is the hermitian transpose of C. If C is real then $C^* = C^T$.*

Lemma 2 *Consider the matrices A and C, defined above. If $\tau_n = 1$ then*

$$\boldsymbol{v}^* (C + C^*) \boldsymbol{v} \geq 0, \forall \boldsymbol{v},$$

$$A = A^T, \quad \boldsymbol{v}^* A \boldsymbol{v} \geq 0, \forall \boldsymbol{v}.$$

If in addition γ_1 or γ_2 is nonzero then

$$A = A^T, \quad \boldsymbol{v}^* A \boldsymbol{v} > 0, \forall \boldsymbol{v} \neq 0.$$

Proof: Consider first A and set $\tau_n = 1$, we have

$$A = M + B_e.$$

Since $M^T = M \geq 0$ and $B_e = B_e^T \geq 0$ is diagonal then $A = A^T \geq 0$. We can compute

$$\mathbf{v}^* A \mathbf{v} = \mathbf{v}^* M \mathbf{v} + \frac{\gamma_1}{|\beta_1|} v_0^2 + \frac{\gamma_2}{\beta_2} v_N^2.$$

Note that $\mathbf{v}^* M \mathbf{v} = 0 \equiv \mathbf{v} = const[1, 1, \cdots, 1]^T$ or $\mathbf{v} = 0$. Therefore the condition $\gamma_1 > 0$ or $\gamma_2 > 0$ implies $\mathbf{v}^* A \mathbf{v} > 0$, $\forall \mathbf{v} \neq 0$.

Next we consider C

$$C = B_s - H\Sigma = B_s - H^{1/2}\left(H^{1/2}\Sigma H^{1/2}\right)H^{-1/2}.$$

Since we need to show that the symmetric part $C + C^*$ is positive semi-definite, it is enough to determine the eigenvalues of $H\Sigma$. Note that

$$H\Sigma = H^{1/2}\left(H^{1/2}\Sigma H^{1/2}\right)H^{-1/2}$$

is a similarity transformation. We know that $\Sigma \leq 0$, is a diagonal matrix and $H = H^T > 0$ defines a norm. Therefore $H\Sigma$ has the same eigenvalues as the symmetric negative semi-definite matrix $H^{1/2}\Sigma H^{1/2}$. We can compute

$$\mathbf{v}^*\left(C + C^*\right)\mathbf{v} = \mathbf{v}^*(B_s + B_s^T)\mathbf{v} - \mathbf{v}^*\left(H\Sigma + \Sigma H\right)\mathbf{v} \geq 0.$$

□

We define the discrete inner products

$$\langle \mathbf{v}, \mathbf{w} \rangle := \mathbf{w}^*\mathbf{v}, \quad \langle \mathbf{v}, \mathbf{w} \rangle_H := \mathbf{w}^* H \mathbf{v}, \tag{22}$$

and the corresponding discrete norms

$$\langle \mathbf{v}, \mathbf{v} \rangle := \mathbf{v}^*\mathbf{v}, \quad \langle \mathbf{v}, \mathbf{v} \rangle_H := \mathbf{v}^* H \mathbf{v}. \tag{23}$$

Consider,

$$\langle \mathbf{v}, D\mathbf{w} \rangle_H = \langle \mathbf{v}, -A\mathbf{w} \rangle = \langle -A\mathbf{v}, \mathbf{w} \rangle = \langle D\mathbf{v}, \mathbf{w} \rangle_H.$$

D is self adjoint in $\langle \cdot, \cdot \rangle_H$. Then we define a semi-discrete energy,

$$E_v(t) := \langle \mathbf{v}_t, \mathbf{v}_t \rangle_H + \langle \mathbf{v}, A\mathbf{v} \rangle. \tag{24}$$

$E_v(t)$ is an energy if $E_v(t) \geq 0$, $\forall t > 0$, and if $E_v(t) = 0$ then $\mathbf{v} = const$.

Theorem 3 *Consider the system of ODE's (21) with a homogeneous boundary data $g_1 = 0$, $g_2 = 0$. If there exists $A = A^T \geq 0$, C such that $C + C^* \geq 0$ and $H = H^* > 0$ such that*

$$D = -H^{-1}A \quad B = -H^{-1}C,$$

then

$$E_v(t) := \langle \boldsymbol{v}_t, \boldsymbol{v}_t \rangle_H + \langle \boldsymbol{v}, A\boldsymbol{v} \rangle.$$

is an energy and

$$\sqrt{E_v(t)} \leq \sqrt{E_v(0)} + \int_0^t ||\boldsymbol{F}(\tau)||_H d\tau, \quad 0 \leq \tau \leq t. \tag{25}$$

If $F \equiv 0$ and $C^* + C = 0$ then $E_v(t) = E_v(0)$.

Proof:

$A^T = A \geq 0$ implies that $E_v(t) \geq 0, \quad \forall \mathbf{v}$. If $E_v(t) = 0$, then $\mathbf{v} = const$. Therefore $E_v(t) \geq 0$ is an energy.

To derive the estimate (25) we multiply (21) by $\mathbf{v}_t^* H$, adding the conjugate transpose of the product (referred to as the energy method) leads to

$$\frac{d}{dt} E_v(t) = -\langle (C^* + C)\, \mathbf{v}_t, \mathbf{v}_t \rangle + \langle \mathbf{v}_t, \mathbf{F} \rangle_H + \langle \mathbf{F}, \mathbf{v}_t \rangle_H.$$

We write $E_v(t) = \sqrt{E_v(t)}\sqrt{E_v(t)}$, using the fact $\sqrt{E_v(t)} \geq \|\mathbf{v}_t\|_H$, yields

$$\sqrt{E_v(t)} \frac{d}{dt} \sqrt{E_v(t)} \leq -\frac{1}{2} \langle (C^* + C)\, \mathbf{v}_t, \mathbf{v}_t \rangle + \sqrt{E_v(t)} ||\mathbf{F}||_H.$$

If $E_v(t) > 0$, time-integration yields

$$\sqrt{E_v(t)} \leq \sqrt{E_v(0)} + \int_0^t ||\mathbf{F}(\tau)||_H d\tau.$$

□

The estimate (25) is completely analogous to the continuous estimate (13). We have proved the semi-discrete equivalent of Theorem 2. We conclude that the semi-discrete problem (19) is strictly stable. We note that if data is inhomogeneous and $C + C^* > 0$, a semi-discrete energy estimate similar to (9) can be derived.

3 Central difference time discretization

In this section we derive and analyze time propagating schemes for second order wave equations. We begin with a second order accurate central difference scheme and extend to arbitrary high order accurate schemes in the next section. Consider the initial value problem (26)

$$\mathbf{v}_{tt} = B\mathbf{v}_t + D\mathbf{v} + \mathbf{F}(t), \quad t > 0, \quad \mathbf{v}(0) = \mathbf{u}_0, \quad \mathbf{v}_t(0) = \mathbf{v}_0, \tag{26}$$

where

$$D = -H^{-1}A, \quad B = -H^{-1}C, \quad A^T = A \geq 0, \quad H^* = H > 0, \quad C^* + C \geq 0. \tag{27}$$

(26) models the SBP-SAT, semi-discrete approximation of the second order wave equations, (1) – (3).

3.1 The time-stepping schemes.

We introduce the discrete time variable $t_n = n\triangle t, n \in \mathbb{N}$, where $\triangle t$ is the time-step. The approximation of the solution at time t_n is denoted $\mathbf{v}^n$, $\mathbf{v}(t_n) \approx \mathbf{v}^n$. We will show how to derive $2m$-th order accurate difference approximations of systems (26), of the form

$$\frac{\mathbf{v}^{n+1} - 2\mathbf{v}^n + \mathbf{v}^{n-1}}{\triangle t^2} = \tilde{B}_m \frac{\mathbf{v}^{n+1} - \mathbf{v}^{n-1}}{2\triangle t} + \tilde{D}_m \mathbf{v}^n + \tilde{\mathbf{F}}^n_m. \qquad (28)$$

Accuracy is achieved by systematically eliminating terms in the truncation error. The difficulty lies in ensuring stability.

To prove stability we make following assumptions

$$\begin{array}{ll} i) & \tilde{D}_m = -\tilde{H}_m^{-1}\tilde{A}_m, \\ ii) & \tilde{A}_m = \tilde{A}_m^T \geq 0, \quad \tilde{H}_m^* = \tilde{H}_m > 0, \\ iii) & \tilde{B}_m = -\tilde{H}_m^{-1}\tilde{C}_m, \quad \tilde{C}_m + \tilde{C}_m^* \geq 0. \end{array} \qquad (29)$$

for our approximations, which will be proven later. We can define the discrete quantity $\mathcal{E}_m^{n+1}$,

$$\begin{aligned} \mathcal{E}_m^{n+1} &:= \left\langle \frac{\mathbf{v}^{n+1} - \mathbf{v}^n}{\triangle\, t}, \frac{\mathbf{v}^{n+1} - \mathbf{v}^n}{\triangle\, t} \right\rangle_{\tilde{H}_m} + \left\langle \mathbf{v}^{n+1}, \tilde{A}_m \mathbf{v}^n \right\rangle \\ &= \left\langle \frac{\mathbf{v}^{n+1} - \mathbf{v}^n}{\triangle t}, \left(\tilde{H}_m - \frac{\triangle t^2}{4}\tilde{A}_m\right) \frac{\mathbf{v}^{n+1} - \mathbf{v}^n}{\triangle t} \right\rangle \\ &+ \left\langle \frac{\mathbf{v}^{n+1} + \mathbf{v}^n}{2}, \tilde{A}_m \frac{\mathbf{v}^{n+1} + \mathbf{v}^n}{2} \right\rangle. \end{aligned} \qquad (30)$$

Definition 3 *The discrete quantity $\mathcal{E}_m^{n+1}$ is an energy if*

$$\mathcal{E}_m^{n+1} \geq 0, \quad \forall \boldsymbol{v}^{n+1}, \boldsymbol{v}^n,$$

and

$$\mathcal{E}_m^{n+1} = 0 \implies \boldsymbol{v}^{n+1} = \boldsymbol{v}^n.$$

Let us denote λ_{mj} the eigenvalues of $\tilde{A}_m$ and σ_{mj} the eigenvalues of $\tilde{H}_m$.

Lemma 3 *If the (CFL) condition*

$$\frac{\triangle t^2}{4} \max_j |\lambda_{mj}| < \min_j \sigma_{mj}, \qquad (31)$$

is satisfied, then the quantity $\mathcal{E}_m^{n+1}$ is an energy.

Proof

By assumption (29) ii), $\tilde{A}_m^T = \tilde{A}_m \geq 0$. Celarly, if (31) holds then $\mathcal{E}_m^{n+1} > 0, \quad \forall \quad \mathbf{v}^{n+1} \neq \mathbf{v}^n$. On the other hand if (31) holds then

$$\mathcal{E}_m^{n+1} = 0 \implies \mathbf{v}^{n+1} = \mathbf{v}^n, \quad \forall n \geq 0.$$

□

Note that $\max_j |\lambda_{mj}| \sim 1/h$ and $\min_j \sigma_{mj} \sim h$, therefore (31) implies

$$\triangle t \leq ch,$$

where c is a CFL number that depends on the spatial discrete operator and the underlying physical problem. We will now prove a fully discrete equivalent of Theorem 2 and Theorem 3. The first main result of the present study is

Theorem 4 *Consider (28) under the assumption (29). If the CFL condition (31) is satisfied then the energy (30) satisfies*

$$\sqrt{\mathcal{E}_m^n} \leq \sqrt{\mathcal{E}_m^0} + \alpha_0 \sum_{j=1}^{n} ||\tilde{\boldsymbol{F}}_m^j||\triangle t, \quad \alpha_0 > 0. \tag{32}$$

If $\boldsymbol{F}(t) \equiv 0$ *and* $\tilde{C}_m^* + \tilde{C}_m = 0$, *then problem (28) conserves the energy* $\mathcal{E}_m^n = \mathcal{E}_m^0, \quad \forall n \geq 0$.

Proof

Rewriting (28) as

$$\frac{\mathbf{v}^{n+1} + \mathbf{v}^{n-1}}{\triangle t} = \frac{1}{2}\tilde{B}_m\left(\mathbf{v}^{n+1} - \mathbf{v}^{n-1}\right) + \left(\frac{2}{\triangle t}\mathbf{I} + \triangle t\tilde{D}_m\right)\mathbf{v}^n + \triangle t\tilde{\mathbf{F}}_m^n,$$

and multiplying (3.1) with

$$\left(\frac{\mathbf{v}^{n+1} - \mathbf{v}^{n-1}}{\triangle t}\right)^* \tilde{H}_m,$$

and adding the conjugate transpose of the product we have

$$\left\langle\frac{\mathbf{v}^{n+1} - \mathbf{v}^n}{\triangle t}, \frac{\mathbf{v}^{n+1} - \mathbf{v}^n}{\triangle t}\right\rangle_{\tilde{H}_m} + \left\langle\mathbf{v}^{n+1}, \tilde{A}_m\mathbf{v}^n\right\rangle = \left\langle\frac{\mathbf{v}^n - \mathbf{v}^{n-1}}{\triangle t}, \frac{\mathbf{v}^n - \mathbf{v}^{n-1}}{\triangle t}\right\rangle_{\tilde{H}_m}$$
$$+ \left\langle\mathbf{v}^n, \tilde{A}_m\mathbf{v}^{n-1}\right\rangle - \frac{1}{\triangle t}\left\langle\frac{\mathbf{v}^{n+1} - \mathbf{v}^{n-1}}{2}, \left(\tilde{C}_m^* + \tilde{C}_m\right)\frac{\mathbf{v}^{n+1} - \mathbf{v}^{n-1}}{2}\right\rangle$$
$$+ \triangle t\left\langle\frac{\mathbf{v}^{n+1} - \mathbf{v}^{n-1}}{\triangle t}, \tilde{\mathbf{F}}_m^n\right\rangle_{\tilde{H}_m} + \triangle t\left\langle\tilde{\mathbf{F}}_m^n\frac{\mathbf{v}^{n+1} - \mathbf{v}^{n-1}}{\triangle t}\right\rangle_{\tilde{H}_m}.$$

Dividing through by $\triangle t$ yields

$$\frac{\mathcal{E}_m^{n+1} - \mathcal{E}_m^n}{\triangle\, t} = -\langle \frac{\mathbf{v}^{n+1} - \mathbf{v}^{n-1}}{2\triangle t}, \left(\tilde{C}_m^* + \tilde{C}_m\right) \frac{\mathbf{v}^{n+1} - \mathbf{v}^{n-1}}{2\triangle t} \rangle$$
$$+ \langle \frac{\mathbf{v}^{n+1} - \mathbf{v}^{n-1}}{\triangle t}, \tilde{\mathbf{F}}_m^n \rangle_{\tilde{H}_m} + \langle \tilde{\mathbf{F}}_m^n, \frac{\mathbf{v}^{n+1} - \mathbf{v}^{n-1}}{\triangle t} \rangle_{\tilde{H}_m}.$$

After some algebraic manipulations, we apply Cauchy-Schwarz inequality, use the equivalence of norms and the fact

$$\alpha_0 \sqrt{\mathcal{E}_m^{n+1}} \geq \sqrt{\langle \frac{\mathbf{v}^{n+1} - \mathbf{v}^n}{\triangle t}, \frac{\mathbf{v}^{n+1} - \mathbf{v}^n}{\triangle t} \rangle_{\tilde{H}_m}},$$

where

$$\alpha_0 \geq \frac{\max_j \sigma_{mj}}{\min_j \sigma_{mj} - \frac{\triangle t^2}{4} \max_j |\lambda_{mj}|},$$

and we have

$$\frac{\mathcal{E}_m^{n+1} - \mathcal{E}_m^n}{\triangle t} \leq \alpha_0 \left(\sqrt{\mathcal{E}_m^{n+1}} + \sqrt{\mathcal{E}_m^n}\right) ||\tilde{\mathbf{F}}_m^n||. \tag{33}$$

Expressing

$$\mathcal{E}_m^{n+1} - \mathcal{E}_m^n = \left(\sqrt{\mathcal{E}_m^{n+1}} + \sqrt{\mathcal{E}_m^n}\right)\left(\sqrt{\mathcal{E}_m^{n+1}} - \sqrt{\mathcal{E}_m^n}\right),$$

and assuming $\sqrt{\mathcal{E}_m^{n+1}} + \sqrt{\mathcal{E}_m^n} > 0$, yielding

$$\sqrt{\mathcal{E}_m^{n+1}} \leq \sqrt{\mathcal{E}_m^n} + \alpha_0 \triangle t ||\tilde{\mathbf{F}}_m^n||. \tag{34}$$

After some algebraic manipulations we have

$$\sqrt{\mathcal{E}_m^n} \leq \sqrt{\mathcal{E}_m^0} + \alpha_0 \sum_j^n ||\tilde{\mathbf{F}}_m^j|| \triangle t.$$

Clearly if $\tilde{C}_m + \tilde{C}_m^* = 0$ and $\mathbf{F}(t) = 0$, we have $\mathcal{E}_m^{n+1} = \mathcal{E}_m^n, \forall n \geq 0$. Therefore by Lemma 3 if the CFL condition (31) holds, the discrete problem (28) is stable and has a bounded energy $\mathcal{E}_m^n \geq 0, \quad \forall n \geq 0$. □

We have proved the fully discrete equivalent of Theorem 2 and Theorem 3. If the assumptions (29) and the CFL condition (31) are satisfied, then the approximation (28) is strictly stable and completely mimic the continuous and semi-discrete energies (4 , 8, 24).

In order to turn (28) into a time stepping recipe we would need to know the solutions at two previous time levels. To initialize the scheme we therefore consider the Taylor expansion

$$\mathbf{v}(t+\triangle t)=\mathbf{v}(t)+\triangle t\mathbf{v}_t(t)+\frac{\triangle t^2}{2}\mathbf{v}_{tt}(t)+\frac{\triangle t^3}{6}+\mathbf{v}_{ttt}(t)+\frac{\triangle t^4}{24}\mathbf{v}_{tttt}(t)+\cdots \tag{35}$$

It is possible to remove all higher derivatives in (35) using (26) and obtain an arbitrary accurate approximation of the solution $\mathbf{v}(t)$ at $t=\triangle t$.

3.2 Error bound and convergence

Since we initialize the solution at $t=\triangle t$ with the approximation (35) which is not a solution to the difference equation (28), it is important that errors introduced initially remain bounded. A direct consequence of Theorem 4 is that numerical errors are bounded by the errors in the data. It is not enough that errors are bounded we also want to show that for any $n>0$, errors approach zero as the time step goes to zero, $\triangle t\to 0$,

$$\triangle t\to 0 \implies |e^n|\to 0, \quad \forall n>0.$$

That is numerical solutions converge to the exact solution.

Let us denote $\mathbf{v}^n=\mathbf{v}(n\triangle t)+\mathbf{e}^n$, where $\mathbf{v}(n\triangle t)$ is the exact solution of the differential equation (26). Now substitute $\mathbf{v}(n\triangle t)+\mathbf{e}^n$ in (28) we have

$$\frac{\mathbf{e}^{n+1}-2\mathbf{e}^n+\mathbf{e}^{n-1}}{\triangle t^2}=\tilde{B}_m\frac{\mathbf{e}^{n+1}-\mathbf{e}^{n-1}}{2\triangle t}+\tilde{D}\mathbf{e}^n+\mathcal{T}^{(n)}, \quad \mathbf{e}^0=0, \quad \mathbf{e}^1=C_0\triangle t^{2m+1}. \tag{36}$$

Here $\mathbf{e}^0$, $\mathbf{e}^1$ are the numerical errors at times $t=0$ and $t=\triangle t$. C_0 is the error coefficient resulting from the approximation (35), and $\mathcal{T}^{(n)}$ is the truncation error at $t_n=n\triangle t$. We introduce the energy of the error

$$\mathcal{E}_e^{n+1}:=\langle\frac{\mathbf{e}^{n+1}-\mathbf{e}^n}{\triangle t},\frac{\mathbf{e}^{n+1}-\mathbf{e}^n}{\triangle t}\rangle_{\tilde{H}_m}+\langle\mathbf{e}^{n+1},\tilde{A}_m\mathbf{e}^n\rangle.$$

Lemma 4 *If the CFL condition (31) is satisfied, then*

$$\sqrt{\mathcal{E}_e^n}\le K\left(\triangle t^{2m}+\sum_j^n||\mathcal{T}^{(j)}||\triangle t\right), \quad K>0.$$

Proof:

We can compute

$$\sqrt{\mathcal{E}_e^0}=\sqrt{\langle C_0\triangle t^{2m},C_0\triangle t^{2m}\rangle_{\tilde{H}_m}}\le K_0\triangle t^{2m}, \quad K_0>0.$$

As before the energy method yields

$$\begin{aligned}\sqrt{\mathcal{E}_e^n} &\leq \sqrt{\mathcal{E}_e^0} + \alpha_0 \triangle t \sum_j^n ||\mathcal{T}^{(j)}|| \\ &\leq K \left(\triangle t^{2m} + \sum_j^n ||\mathcal{T}^{(j)}|| \triangle t \right).\end{aligned} \tag{37}$$

□

It remains to construct the modified operators $\tilde{B}_m$ and $\tilde{D}_m$ and verify that the assumptions (29) hold. We will begin with a second order accurate time-marching scheme ($m = 1$) and proceed to higher order approximations.

3.3 Second order accurate approximation

A second order accurate approximation of (26) is achieved by using

$$\tilde{B}_1 = B, \quad \tilde{D}_1 = D.$$

By (27) the assumptions (29) are satisfied and Theorem 4 is directly applicable.

4 Higher order approximations and the modified equation approach

In order to obtain higher order accurate (in time) approximations, we use the well-known modified equation approach, [11, 12, 3, 10]. Now consider the central finite difference approximations of the first derivative and second derivative of $\mathbf{v}$, i.e. $\mathbf{v}_t$ and $\mathbf{v}_{tt}$ and their corresponding Taylor expansions,

$$\frac{\mathbf{v}^{n+1} - 2\mathbf{v}^n + \mathbf{v}^{n-1}}{\triangle t^2} = \mathbf{v}_{tt} + \frac{\triangle t^2}{12}\mathbf{v}_{tttt} + \frac{\triangle t^4}{360}\mathbf{v}_{tttttt} + \cdots + O(\triangle t^{2m}), \tag{38}$$

$$\frac{\mathbf{v}^{n+1} - \mathbf{v}^{n-1}}{2\triangle t} = \mathbf{v}_t + \frac{\triangle t^2}{6}\mathbf{v}_{ttt} + \frac{\triangle t^4}{120}\mathbf{v}_{ttttt} + \cdots + O(\triangle t^{2m}). \tag{39}$$

We can eliminate all higher derivatives using (26), that is,

$$\begin{aligned}
&\mathbf{v}_{tt} = B\mathbf{v}_t + D\mathbf{v} + F, \\
&\mathbf{v}_{ttt} = (B^2 + D)\mathbf{v}_t + BD\mathbf{v} + BF + F_t, \\
&\mathbf{v}_{tttt} = ((B^2 + D)B + BD)\mathbf{v}_t + (B^2 + D)D\mathbf{v} + (B^2 + D)F + BF_t + F_{tt}, \\
&\mathbf{v}_{ttttt} = ((B^2 + D)B + B^2D)B + ((B^2 + D)D)\mathbf{v}_t + ((B^2 + D)B + BD)D\mathbf{v} \\
&\qquad + ((B^2 + D)B + BD)F + (B^2 + D)F_t + BF_{tt} + F_{ttt}
\end{aligned}$$

These expressions can be written in a more compact form

$$
\begin{aligned}
\frac{d^k \mathbf{v}}{dt^k} =& B_k \mathbf{v}_t + D_k \mathbf{v} + F_k, \quad B_{k+1} = B_k B + D_k, \quad D_{k+1} = B_k D, \\
F_k =& \sum_{j=1}^{k-1} B_j \frac{d^{k-(j+1)}}{dt^{k-(j+1)}} F, \quad k = 2, 3, \cdots, \quad B_1 = I, \quad B_2 = B, \quad D_2 = D.
\end{aligned} \tag{40}
$$

We now replace all high (even) order derivatives appearing in (38) by (40) yielding

$$
\begin{aligned}
\frac{\mathbf{v}^{n+1} - 2\mathbf{v}^n + \mathbf{v}^{n-1}}{\triangle t^2} &= (B\mathbf{v}_t + D\mathbf{v} + F) + 2\sum_{k=2}^{m} \frac{(\triangle t)^{(2k-2)}}{(2k)!} \left(B_{2k}\mathbf{v}_t + D_{2k}\mathbf{v} + F_{2k}\right) \\
&= B\mathbf{v}_t + 2\sum_{k=2}^{m} \frac{(\triangle t)^{(2k-2)}}{(2k)!} B_{2k}\mathbf{v}_t + \left(D + 2\sum_{k=2}^{m} \frac{(\triangle t)^{(2k-2)}}{(2k)!} D_{2k}\right)\mathbf{v} \\
&+ \left(F + 2\sum_{k=2}^{m} \frac{(\triangle t)^{(2k-2)}}{(2k)!} F_{2k}\right) + O((\triangle t)^{2m}).
\end{aligned} \tag{41}
$$

Also using (40) we eliminate all high (odd) order derivatives appearing in (39)

$$
\begin{aligned}
\frac{\mathbf{v}^{n+1} - \mathbf{v}^{n-1}}{2\triangle t} &= \mathbf{v}_t + \sum_{k=2}^{m} \frac{(\triangle t)^{(2k-2)}}{(2k-1)!} \left(B_{2k-1}\mathbf{v}_t + D_{2k-1}\mathbf{v} + F_{2k-1}\right) \\
&= \mathbf{v}_t + \sum_{k=2}^{m} \frac{(\triangle t)^{(2k-2)}}{(2k-1)!} B_{2k-1}\mathbf{v}_t + \sum_{k=2}^{m} \frac{(\triangle t)^{(2k-2)}}{(2k-1)!} D_{2k-1}\mathbf{v} \\
&+ \sum_{k=2}^{m} \frac{(\triangle t)^{(2k-2)}}{(2k-1)!} F_{2k-1} + O((\triangle t)^{2m}).
\end{aligned}
$$

Rearranging the above expression we have

$$
\begin{aligned}
\mathbf{v}_t = &\frac{\mathbf{v}^{n+1} - \mathbf{v}^{n-1}}{2\triangle t} - \sum_{k=2}^{m} \frac{(\triangle t)^{(2k-2)}}{(2k-1)!} B_{2k-1}\mathbf{v}_t - \sum_{k=2}^{m} \frac{(\triangle t)^{(2k-2)}}{(2k-1)!} D_{2k-1}\mathbf{v} \\
&- \sum_{k=2}^{m} \frac{(\triangle t)^{(2k-2)}}{(2k-1)!} F_{2k-1} + O((\triangle t)^{2m}).
\end{aligned} \tag{42}
$$

It is possible to construct a time-stepping scheme of arbitrary order of accuracy using (41) and (42). We will start with the fourth order scheme.

4.1 A fourth order scheme

To begin, we ignore fourth order terms in (41) yielding,

$$\begin{aligned}\frac{\mathbf{v}^{n+1}-2\mathbf{v}^{n}+\mathbf{v}^{n-1}}{\triangle t^2} &= B_2\mathbf{v}_t + \frac{(\triangle t)^2}{12}B_4\mathbf{v}_t + \left(D_2 + \frac{(\triangle t)^2}{12}D_4\right)\mathbf{v} \\ &+ \left(F + \frac{(\triangle t)^2}{12}F_4\right).\end{aligned} \tag{43}$$

To construct a fourth order scheme, we will first obtain a fourth order approximation of the first order derivative $\mathbf{v}_t$ corresponding to the coefficient B_2. We use (42), replace the derivative $\mathbf{v}_t$ corresponding to the coefficient B_3 with a standard second order approximation and we have

$$\mathbf{v}_t = \frac{\mathbf{v}^{n+1}-\mathbf{v}^{n-1}}{2\triangle t} - \frac{\triangle t^2}{6}B_3\frac{\mathbf{v}^{n+1}-\mathbf{v}^{n-1}}{2\triangle t} - \frac{\triangle t^2}{6}D_3\mathbf{v}^n - \frac{\triangle t^2}{6}F_3 + O(\triangle t^4). \tag{44}$$

The first order derivative $\mathbf{v}_t$ corresponding to the coefficient B_4 is then replaced by a standard second order approximation yielding

$$\frac{\mathbf{v}^{n+1}-2\mathbf{v}^{n}+\mathbf{v}^{n-1}}{\triangle\, t^2} = \tilde{B}_2\frac{\mathbf{v}^{n+1}-\mathbf{v}^{n-1}}{2\,\triangle\, t} + \tilde{D}_2\mathbf{v}^n + \tilde{F}_2^n, \tag{45}$$

where

$$\begin{aligned}\tilde{B}_2 &= B_2 + \frac{\triangle t^2}{12}\left(B_4 - 2B_2B_3\right),\\ \tilde{D}_2 &= D_2 + \frac{\triangle t^2}{12}\left(D_4 - 2B_2D_3\right),\\ \tilde{F}_2^n &= F + \frac{\triangle t^2}{12}\left(\left(B_3 - 2B_2^2\right)F - B_2F_t + F_{tt}\right).\end{aligned}$$

We use (40)

$$\begin{aligned}&B_2 = B, \quad D_2 = D,\\ &B_3 = B^2 + D, \quad D_3 = BD,\\ &B_4 = \left(B^2 + D\right)B + BD, \quad D_4 = B^2D + D^2,\end{aligned}$$

to obtain

$$\begin{aligned}\tilde{B}_2 &= B - \frac{\triangle t^2}{12}\left(B^3 + BD - DB\right),\\ \tilde{D}_2 &= D + \frac{\triangle t^2}{12}\left(D^2 - B^2D\right).\end{aligned}$$

Then using (27): $B = -H^{-1}C$, $D = -H^{-1}A$, we have

$$\tilde{D}_2 = -H^{-1}\left(H - \frac{\triangle t^2}{12}\left(A + CH^{-1}C\right)\right)H^{-1}A. \tag{46}$$

We set

$$\tilde{A}_2 = A, \quad \tilde{H}_2 = H\left(H - \frac{\triangle t^2}{12}\left(A + CH^{-1}C\right)\right)^{-1} H.$$

Lemma 5 *If A is symmetric and positive semi-definite, then $\tilde{A}_2$ is also symmetric and positive semi-definite.*

Proof:

Set $\tilde{A}_2 = A$. By (27), $A = A^T \geq 0$, the Lemma therefore holds. □

Let us denote λ_j the eigenvalues of A and σ_j the eigenvalues of H. For $\tilde{H}_2$ we have

Lemma 6 *Assume $C = C^*$ or $C + C^* = 0$, if the condition*

$$\frac{\triangle t^2}{12}\left(\max_j |\lambda_j| + |C|^2_{H^{-1}}\right) < \min_j \sigma_j, \tag{47}$$

holds, then $\tilde{H}_2 = \tilde{H}_2^*$, and positive definite, $\tilde{H}_2 = \tilde{H}_2^* > 0$.

Proof:

By taking the hermitian transpose of $\tilde{H}_2$ we have

$$\tilde{H}_2^* = H\left(H - \frac{\triangle t^2}{12}\left(A + C^*H^{-1}C^*\right)\right)^{-1} H.$$

Clearly if $C = C^*$ or $C + C^* = 0$ then $\tilde{H}_2 = \tilde{H}_2^*$. If the condition (47) holds then $\tilde{H}_2$ is positive definite. □

Next we consider $\tilde{B}_2$,

$$\tilde{B}_2 = -H^{-1}\left(C - \frac{\triangle t^2}{12}\left(CH^{-1}CH^{-1}C - CH^{-1}A + AH^{-1}C\right)\right).$$

To write $\tilde{B}_2$ in the form of (29), iii), i.e. $\tilde{B}_2 = -\tilde{H}_2^{-1}\tilde{C}_2$, we write

$$\tilde{B}_2 = \tilde{H}_2^{-1}\left(\tilde{H}_2\tilde{B}_2\right).$$

We set

$$\begin{aligned}
\tilde{C}_2 &= -\left(\tilde{H}_2\tilde{B}_2\right) \\
&= C + \frac{\triangle t^2}{12} H\left(H - \frac{\triangle t^2}{12}\left(A + CH^{-1}C\right)\right)^{-1} HH^{-1}CH^{-1}A \\
&= C + \frac{\triangle t^2}{12}\left(\tilde{H}_2 H^{-1}CH^{-1}A\right).
\end{aligned}$$

Lemma 7 *If $C = C^* \geq 0$ or $C + C^* = 0$ and (47) holds then*

$$\tilde{C}_2^* + \tilde{C}_2 \geq 0.$$

Proof:

In general the discrete operator A is symmetric and positive semi-definite. Let $\mathcal{V}$ be the set of eigenvectors corresponding to a zero eigenvalue of A, that is

$$\mathcal{V} := \{\mathbf{v}_0 : A\mathbf{v}_0 = 0\}$$

For our model problem (21) the corresponding eigenvector is

$$\mathcal{V} = \{[1, 1, \cdots, 1]^T\}.$$

Clearly

$$\mathbf{v}_0^* \left(\tilde{C}_2^* + \tilde{C}_2\right) \mathbf{v}_0 = \mathbf{v}_0^* \left(C^* + C\right) \mathbf{v}_0 \geq 0, \quad \forall \mathbf{v}_0 \in \mathcal{V}.$$

Now let $\mathbf{v} \in \mathbb{C}^n \setminus \{\mathcal{V}, \mathbf{0}\}$, where $\mathbf{0}$ is the zero vector. We can calculate

$$\begin{aligned}\mathbf{v}^* \left(\tilde{C}_2 + \tilde{C}_2^*\right) \mathbf{v} &= \mathbf{v}^* \left(C + C^*\right) \mathbf{v} \\ &+ \frac{\triangle t^2}{12} \mathbf{v}^* \tilde{H}_2^{1/2} \left(\tilde{H}_2^{1/2} Q \tilde{H}_2^{-1/2} + \tilde{H}_2^{-1/2} Q^* \tilde{H}_2^{1/2}\right) \tilde{H}_2^{1/2} \mathbf{v},\end{aligned}$$

where $Q = H^{-1}CH^{-1}A$. We need to show that the symmetric part, $\tilde{C}_2 + \tilde{C}_2^*$, is positive semi-definite. It is enough to show that the real parts of the eigenvalues of Q are nonnegative, $\Re\lambda_i(Q) \geq 0$.

Consider first $C = C^* \geq 0$. If $A = A^T > 0$ then the eigenvalues $\lambda_i(Q)$ are purely real and nonnegative. Therefore, the matrix $\tilde{C}_2 + \tilde{C}_2^*$ is symmetric and positive semi-definite. Note that if $C = C^* > 0$ and $A = A^T \geq 0$ then the eigenvalues $\lambda_i(Q)$ are purely real and nonnegative, the matrix $\tilde{C}_2 + \tilde{C}_2^*$ is also symmetric and positive semi-definite.

Since in general $A = A^T \geq 0$ and $C = C^* \geq 0$ we consider

$$Q(\epsilon) = H^{-1}CH^{-1}A_\epsilon,$$

where

$$A_\epsilon = A + \epsilon I, \quad \epsilon > 0.$$

Here I is the identity matrix, the matrix A_ϵ is symmetric and positive definite. We define

$$\lambda_i(Q) := \lim_{\epsilon \longrightarrow 0} \lambda_i(Q(\epsilon)).$$

Since the matrix A_ϵ is symmetric and positive definite, we have

$$\lambda_i\left(Q(\epsilon)\right) \geq \lambda_{\min}\big(H^{-1}CH^{-1}\big)\lambda_i(A_\epsilon) \geq \epsilon\lambda_{\min}\big(H^{-1}CH^{-1}\big).$$

We know that the eigenvalues $\lambda_i(Q(\epsilon))$ depend continuously on the coefficients, we obtain

$$\lambda_i(Q) = \lim_{\epsilon \to 0} \lambda_i(Q(\epsilon)) \geq 0.$$

Therefore, if $A = A^T \geq 0$ and $C = C^* \geq 0$, then

$$\mathbf{v}^* \left(\tilde{C}_2 + \tilde{C}_2^* \right) \mathbf{v} \geq 0.$$

Now consider the case $C + C^* = 0$. We can compute

$$Q(\epsilon) = A_\epsilon^{-1/2} \left(A_\epsilon^{1/2} H^{-1} C H^{-1} A_\epsilon^{1/2} \right) A_\epsilon^{1/2}.$$

$Q(\epsilon)$ is similar to the anti-symmetric matrix $A_\epsilon^{1/2} H^{-1} C H^{-1} A_\epsilon^{1/2}$. The eigenvalues $\lambda_i(Q)$ are purely imaginary and we have

$$\mathbf{v}^* \left(\tilde{C}_2 + \tilde{C}_2^* \right) \mathbf{v} = 0.$$

□

We are now ready to state the main result.

Theorem 5 *Consider (26) where the coefficients satisfy (27), and the fully discrete problem (45) where* $\tilde{B}_2$, $\tilde{D}_2$ *and* $\tilde{F}_2^n$ *are given by*

$$\begin{aligned}
\tilde{B}_2 &= B - \frac{\triangle t^2}{12} \left(B^3 + BD - DB \right), \\
\tilde{D}_2 &= D + \frac{\triangle t^2}{12} \left(D^2 - B^2 D \right), \\
\tilde{F}_2^n &= F + \frac{\triangle t^2}{12} \left(\left(D - B^2 \right) F - BF_t + F_{tt} \right).
\end{aligned}$$

If the conditions of Lemma 7 are fulfilled, and both conditions

$$\frac{\triangle t^2}{12} \left(\max_j |\lambda_j| + |C|_{H^{-1}}^2 \right) < \min_j \sigma_j,$$

and

$$\frac{\triangle t^2}{4} \max_j |\lambda_j| < \min_j \sigma_j,$$

hold, then the fully discrete problem is a 4th order approximation and the energy (30) satisfies

$$\sqrt{\mathcal{E}_2^n} \leq \sqrt{\mathcal{E}_2^0} + \alpha_0 \sum_{j=1}^{n} ||\tilde{\boldsymbol{F}}_2^j|| \triangle t, \quad \alpha_0 > 0. \tag{48}$$

By Lemmas 5, 6 and 7 the assumptions (29) are satisfied. Therefore the proof of Theorem 5 follows directly from Theorem 4.

We note that the scheme can be extended to arbitrary order of accuracy. In the Appendix we have constructed and analyzed the sixth order accurate scheme.

To initialize the scheme we use a Taylor expansion of the initial solution about $t = \triangle t$. A high order approximation of the solution at $t_1 = \triangle t$ yields

$$\begin{aligned}\mathbf{v}(\triangle t) &= \mathbf{v}(0) + \triangle t \mathbf{v}_t(0) + \frac{\triangle t^2}{2}\left(B\mathbf{v}_t(0) + D\mathbf{v}(0) + F(0)\right)\\ &+ \sum_{k=3}^{2m} \frac{(\triangle t)^k}{k!}\left(B_k \mathbf{v}_t(0) + D_k \mathbf{v}(0) + F_k(0)\right) + O(\triangle t^{2m+1}).\end{aligned} \tag{49}$$

We conclude this section by noting hidden but important observations. The stability of the schemes depend on $|B|_H$ and $|D|_H$. If the ODE (5) corresponds to an SBP-SAT approximation of the wave equation we have $|H| \sim h$, where h is the spatial grid-size and $|B|_H \le \kappa \ge 0$, $|D|_H \sim 1/h$. We see that as $h \to 0$, $|B|_H$ remains bounded while $|D|_H \sim 1/h \to \infty$. For reasonably small mesh-sizes the stability of the algorithm essentially depends on $|D|_H$. For the fourth order scheme we see that if

$$\frac{\triangle t^2}{12}\left(\frac{c_0^2}{h} + \kappa^2\right) \le h,$$

then the corresponding $\tilde{H}$-norm is positive definite and $\tilde{B} \le 0$. Here c_0 is the maximum wave speed. We also have

$$\triangle\, t \le \sqrt{\frac{3}{c_0^2 + \kappa^2 h}}\, 2h > \sqrt{\frac{1}{c_0^2 + \kappa^2 h}}\, 2h,$$

where

$$\triangle\, t \le \sqrt{\frac{1}{c_0^2 + \kappa^2 h}}\, 2h,$$

is the CFL for the second order accurate scheme. We see that with increasing accuracy the CFL improves and we can use larger time steps.

5 Numerical tests

In this section we present some numerical examples. We begin by discretizing the one dimensional wave equation (6) in the domain, $[-1, 1]$. In order to make the errors resulting from the spatial approximations negligible, we have used a 6-th order accurate SBP operator (SBP6 – 6-th order in the interior with lower order boundary closures) for the spatial derivatives [5]. Boundary conditions are imposed weakly, leading to a highly accurate and asymptotically stable semi-discrete problem.

5.1 Non-conducting medium and homogeneous data

In the first set of experiments, we consider a non-conducting medium, $\sigma = 0$, with vanishing forcing, $f(x,t) = 0$, and homogeneous boundary data. We use the initial data

$$u(x,0) = \exp(-x^2/0.01), \quad u_t(x,0) = 0. \tag{50}$$

In the absence of boundaries the wave equation has the exact solution

$$u(x,t) = \frac{1}{2}\exp(-(x+t)^2/0.01) + \frac{1}{2}\exp(-(x-t)^2/0.01). \tag{51}$$

First, we set the radiation boundary conditions

$$\begin{aligned} u_t - u_x = 0, &\quad x = -1, \\ u_t + u_x = 0, &\quad x = 1. \end{aligned} \tag{52}$$

In this case the damping term B, is non-zero only at the boundaries. Here, the penalty term is set to $\tau_n = 1$, by Lemma 2 and Theorem 3 the semi-discrete problem is strictly stable. We compute the solution until $t = 1$, for different resolutions. The time evolution of the numerical solution is displayed in Figure 1. At $t = 1$, half of the pulses have left the domain and the two peaks of the pulses are centered on the boundaries $x = -1, 1$. We have used the 4-th and 2-nd order accurate conservative schemes (derived in this paper) and 4-th order explicit Runge-Kutta method. The time step is $\triangle t = 0.1h$, where h is the spatial grid-size. We have plotted the numerical errors as a function of time for the various schemes in Figure 2. In Table 1, the errors at the final time are displayed. We see that the 4-th order scheme and the 4-th order Runge-Kutta scheme remain very accurate. For the 4-th order schemes, the spatial errors dominate and we recover the theoretical order of accuracy of the SBP operator, see [5]. In the second order case, the errors due to the time discretizations dominate, it is not surprising that the solution remains second order accurate.

In order to investigate efficiency, we measure the CPU-time for each computation. Results are plotted in Figure 3. At moderate error tolerance the 2-nd order scheme is efficient. For a lower tolerance, higher order methods are more efficient. We also note that for the higher order methods: the work needed by the Runge-Kutta scheme to advance the solution one step in time is the double of the time needed by our 4-th order scheme.

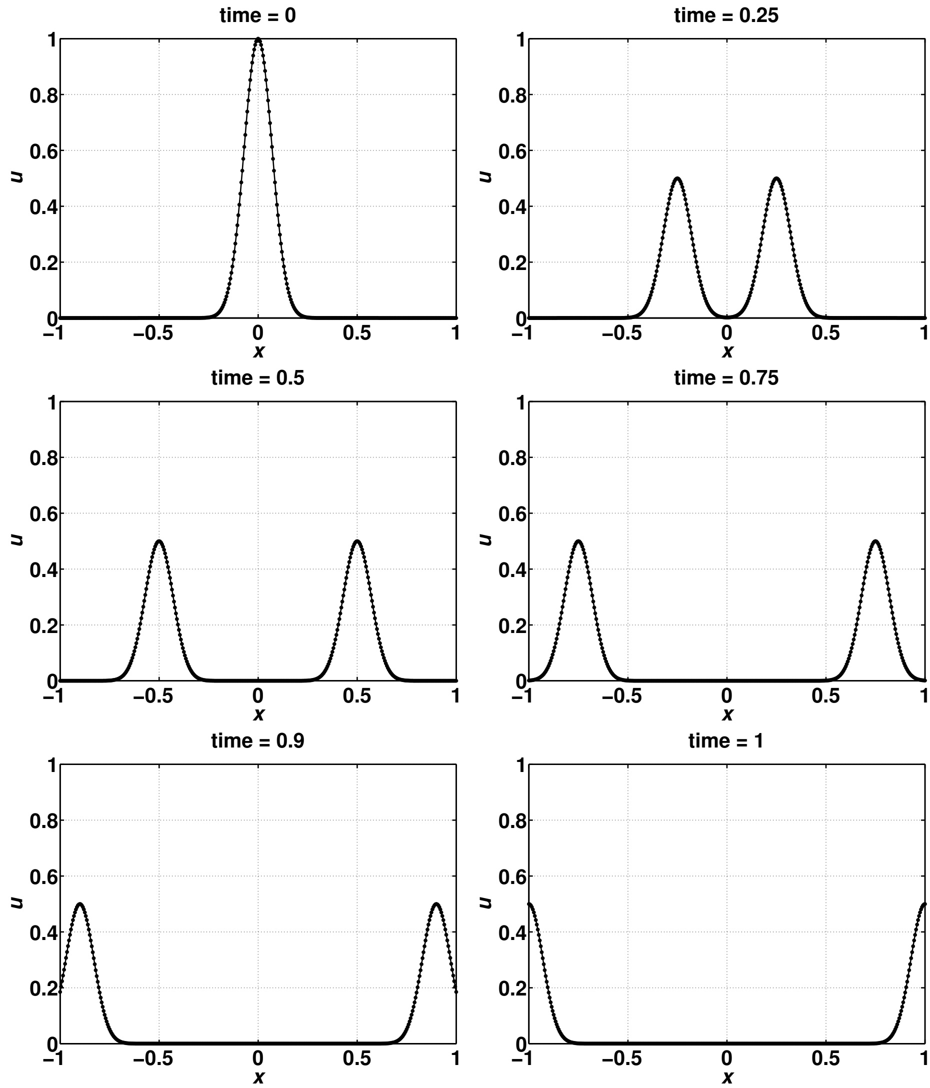

Figure 1: *The snapshots of the numerical solution in a non-conducting medium with homogeneous forcing and boundary data*

In the second experiment we impose homogeneous Neumann boundary conditions

$$\begin{aligned} u_x &= 0, \quad x = -1, \\ u_x &= 0, \quad x = 1, \end{aligned} \tag{53}$$

such that the discrete energy is conserved. We set the penalty $\tau_n = 1$. We compute the solution using the 2-nd order and 4-th order schemes, and measure the discrete energy. In Figure 4, we have plotted the deviation of the discrete energy from the initial energy. As predicted by the analysis the discrete energy is conserved.

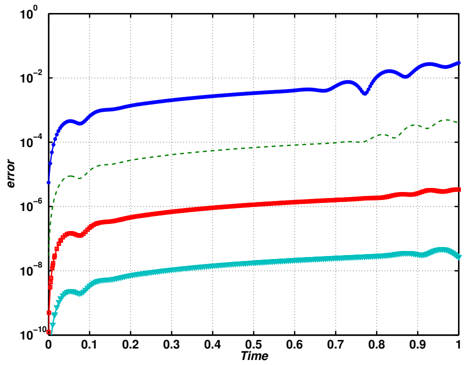

(a) fourth order accurate time propagator

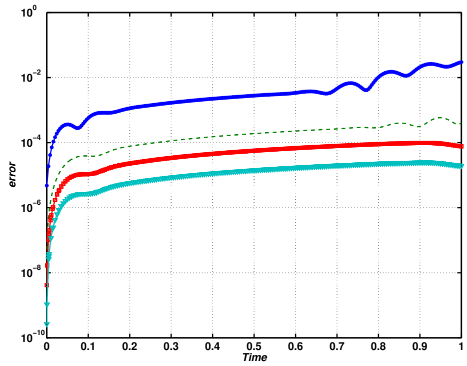

(b) second order accurate time propagator

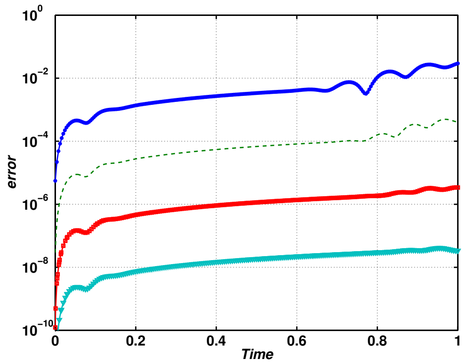

(c) fourth order Runge-Kutta

Figure 2: *Numerical error as a function of time, for the sixth order accurate SBP operator in a non-conducting medium with a homogeneous forcing and boundary data. Each curve in the figures is the numerical error corresponding to the refinement levels,* $h = 0.04, 0.02, 0.01, 0.005, 0.0025$.

Mesh-size (h)	SBP6					
	4-th Order		2-nd Order		RK4	
	$\|\mathbf{error}\|_\infty$	**rate**	$\|\mathbf{error}\|_\infty$	**rate**	$\|\mathbf{error}\|_\infty$	**rate**
0.04	2.9408×10^{-2}	–	2.9919×10^{-2}	–	2.9406×10^{-2}	–
0.02	4.0760×10^{-4}	6.1729	3.9645×10^{-4}	6.2378	4.0769×10^{-4}	6.1725
0.01	3.3624×10^{-6}	6.9215	7.6895×10^{-5}	2.3662	3.4072×10^{-6}	6.9027
0.005	2.6851×10^{-8}	6.9684	1.9532×10^{-5}	1.9771	3.3857×10^{-8}	6.6530

Table 1: Numerical error as a function of grid-size h, for the sixth order accurate SBP operator in a non-conducting medium with a homogeneous forcing and boundary data

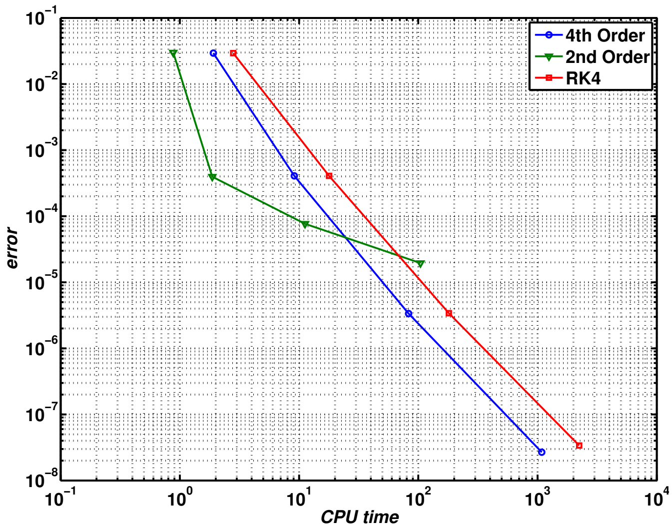

Figure 3: *CPU time versus error in a non-conducting media with homogeneous forcing and boundary data .*

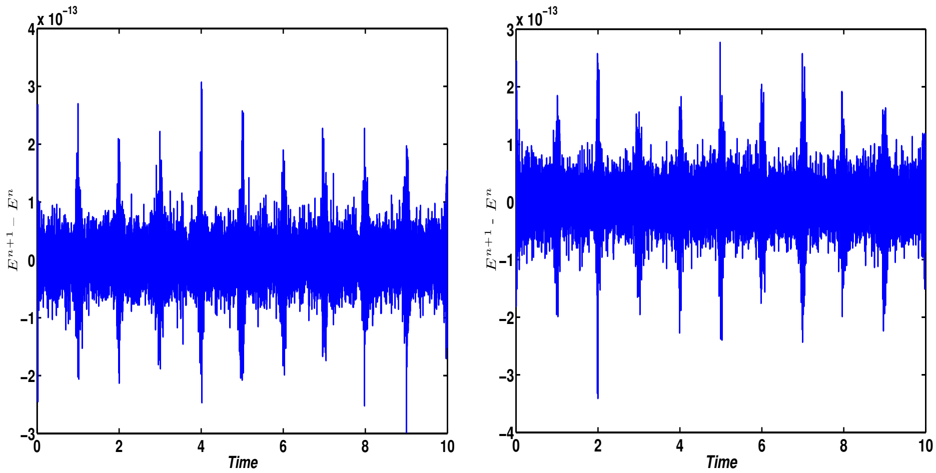

(a) fourth order

(b) second order

Figure 4: *Conservation of the discrete energy. Note the scale* $\sim 10^{-13}$ *in the vertical axis.*

5.2 Conducting medium and inhomogeneous data

In the final set of experiments, we consider the wave equation in a conducting medium, $\sigma = -1$. We chose the initial data to match the exact solution

$$U(x,t) = \cos(\pi t)\sin(n\pi x). \tag{54}$$

We set $n = 5/2$, so that the solution is smooth and it can be easily well-resolved. Using the exact solution (54) we construct a compatible forcing function, $f(x,t)$. We set boundary conditions of the form

$$\begin{aligned} \beta_1 u_x + \gamma_1 u = g_1, \qquad & x = -1, \\ \beta_2 u_x + \gamma_2 u = g_2, \qquad & x = 1. \end{aligned} \tag{55}$$

Compare (55) to (17), and set $\alpha_1 = \alpha_2 = 0$, $\beta_1 = -1$, $\beta_2 = 1$, and $\gamma_1 = \gamma_2 = 1$. The boundary data is $g_1(t) = U - U_x$, $g_2(t) = U + U_x$. As before, we discretize in space using a sixth order SBP operator. Since $\alpha_i = 0$, $\gamma_i > 0$, $\beta_1 < 0$, $\beta_2 > 0$, by Lemma 2 and Theorem 3, $\tau_n = 1$ ensures strict stability. Numerical experiments are performed using our second, fourth and sixth order schemes, and the fourth order classical Runge-Kutta scheme. The time step is $\triangle t = 0.1h$, where h is the spatial grid-size. Numerical errors are displayed in Figure 5 and Tables 2 and 3. We see that our numerical scheme formulated for the second order system remains very accurate and efficient. The Runge-Kutta scheme has lost its accuracy due to the time-dependent boundary data. Secondly, the time needed for the Runge-Kutta scheme to advance the solution one step in time has increased (by a factor of 10) dramatically. Note that there is a possible remedy to the loss of accuracy of the Runge-Kutta scheme, see [13, 14], which also leads to a reduced CFL condition. However, in a more complicated scenario the modified Runge-Kutta scheme may be non-trivial to implement.

Note that at small mesh-sizes $h < 0.005$ the approximation errors are small and the rounding errors dominate. By increasing the spatial frequency to $n = 5.5$ in (54), the approximation errors dominate and we recover the theoretical order of accuracy for the smallest mesh-size $h = 0.0025$, see Table 4 and Figure 6.

	6-th Order		4-th Order	
h	$\lVert$**error**$\rVert_\infty$	**rate**	$\lVert$**error**$\rVert_\infty$	**rate**
0.04	1.7707×10^{-5}	–	1.7706×10^{-5}	–
0.02	2.5934×10^{-7}	6.0932	2.5931×10^{-7}	6.0934
0.01	3.1745×10^{-9}	6.3522	3.1737×10^{-9}	6.3524
0.005	3.9769×10^{-11}	6.3188	3.9251×10^{-11}	6.3373
0.0025	3.3387×10^{-11}	0.2523	3.2872×10^{-11}	0.2558

Table 2: Numerical error as a function of grid-size h, for the sixth order accurate SBP operator, in a conducting medium with time-dependent boundary data and spatial frequency $n = 2.5$

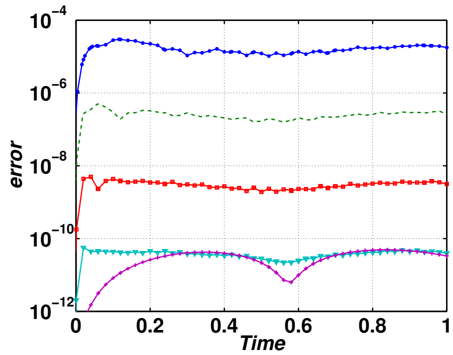

(a) numerical error for the sixth order scheme

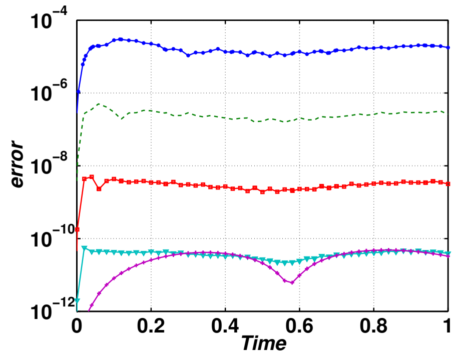

(b) numerical error for the fourth order scheme

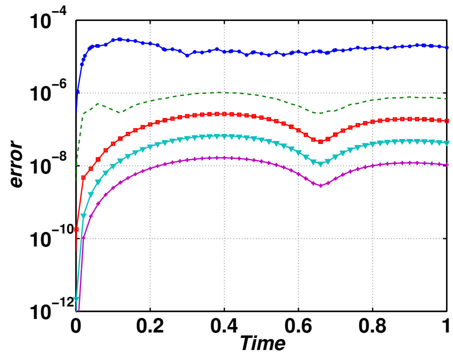

(c) numerical error for the second order scheme

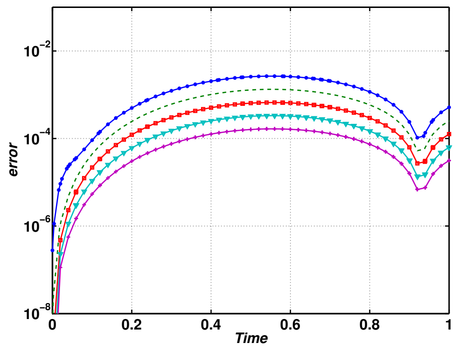

(d) numerical error for the fourth order Runge-Kutta scheme

Figure 5: *Numerical error as a function of grid-size h, for the sixth order accurate SBP operator, in a conducting medium with time-dependent boundary data and spatial frequency $n = 2.5$. Each curve in the figures is the numerical error corresponding to the refinement levels,* $h = 0.04, 0.02, 0.01, 0.005, 0.0025$.

$\triangle x$	2-nd Order		RK4	
	$\|\textbf{error}\|_\infty$	**rate**	$\|\textbf{error}\|_\infty$	**rate**
0.04	1.7600×10^{-5}	–	5.1521×10^{-4}	–
0.02	6.8775×10^{-7}	4.6775	2.5354×10^{-4}	1.0229
0.01	1.7010×10^{-7}	2.0155	1.2609×10^{-4}	1.0078
0.005	4.2673×10^{-8}	1.9950	6.2878×10^{-5}	1.0038
0.0025	1.0640×10^{-8}	2.0038	3.1398×10^{-5}	1.0019

Table 3: Numerical error as a function of grid-size h, for the sixth order accurate SBP operator, in a conducting medium with time-dependent boundary data and spatial frequency $n = 2.5$

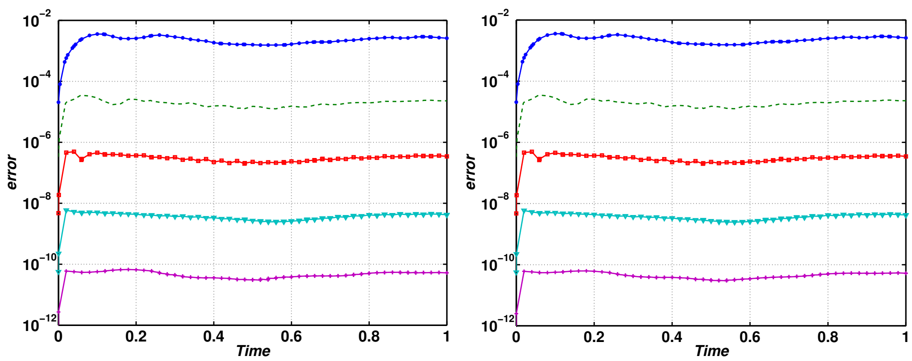

(a) numerical error for the sixth order scheme (b) numerical error for the fourth order scheme

Figure 6: *Numerical error as a function of grid-size* h*, for the sixth order accurate SBP operator, in a conducting medium with time-dependent boundary data and spatial frequency* $n = 5.5$*. Each curve in the figures is the numerical error corresponding to the refinement levels,* $h = 0.04, 0.02, 0.01, 0.005, 0.0025$*.*

h	6-th Order error	rate	4-th Order error	rate
0.04	2.6000×10^{-3}	–	2.6000×10^{-3}	–
0.02	2.2947×10^{-5}	6.8253	2.2947×10^{-5}	6.8252
0.01	3.4614×10^{-7}	6.0508	3.4609×10^{-7}	6.0510
0.005	4.1368×10^{-9}	6.3866	4.1336×10^{-9}	6.3877
0.0025	5.193×10^{-11}	6.3157	5.2452×10^{-11}	6.3002

Table 4: Numerical error as a function of grid-size h, for the sixth order accurate SBP operator, in a conducting medium with time-dependent boundary data and spatial frequency $n = 5.5$

6 Conclusions

We have presented in this paper a hierarchy of explicit time propagating schemes for second order wave equations when the spatial approximations are obtained with SBP-SAT schemes. In the semi-discrete setting energy techniques can be used to prove stability. The time discretization starts with a second order central difference scheme, then using the modified equation approach we derive arbitrary high order accurate and fully explicit time marching schemes. We have proved that if a CFL condition is satisfied the fully discrete problem is energy stable. With increasing accuracy the CFL improves rendering the scheme very accurate and efficient. Numerical examples are also presented showing the stability, accuracy and efficiency of the proposed schemes.

Appendix

A sixth order scheme

By ignoring the sixth order terms in (41) we have,

$$\begin{aligned}\frac{\mathbf{v}^{n+1}-2\mathbf{v}^{n}+\mathbf{v}^{n-1}}{\triangle t^2} &= B_2\mathbf{v}_t + \frac{(\triangle t)^2}{12}B_4\mathbf{v}_t + \frac{(\triangle t)^4}{360}B_6\mathbf{v}_t \\ &+ \left(D_2 + \frac{(\triangle t)^2}{12}D_4 + \frac{(\triangle t)^4}{360}D_6\right)\mathbf{v} \\ &+ \left(F + \frac{(\triangle t)^2}{12}F_4 + \frac{(\triangle t)^4}{360}F_6\right).\end{aligned} \tag{56}$$

Now, we need a sixth order approximation of the first order derivative $\mathbf{v}_t$ corresponding to the coefficient B_2, a fourth order approximation of the first order derivative $\mathbf{v}_t$ corresponding to the coefficient B_4 and a second order approximation of the first order derivative $\mathbf{v}_t$ corresponding to the coefficient B_6. The fourth order approximation is given by (44), for the sixth order approximation we use (42) recursively yielding

$$\begin{aligned}\mathbf{v}_t = &\frac{\mathbf{v}^{n+1}-\mathbf{v}^{n-1}}{2\triangle t} - \frac{\triangle t^2}{6}B_3\left(\frac{\mathbf{v}^{n+1}-\mathbf{v}^{n-1}}{2\triangle t} - \frac{\triangle t^2}{6}B_3\frac{\mathbf{v}^{n+1}-\mathbf{v}^{n-1}}{2\triangle t}\right) \\ &+ \frac{\triangle t^2}{6}B_3\left(\frac{\triangle t^2}{6}D_3\mathbf{v}^n + \frac{\triangle t^2}{6}F_3\right) - \frac{\triangle t^4}{120}B_5\frac{\mathbf{v}^{n+1}-\mathbf{v}^{n-1}}{2\triangle t} - \frac{\triangle t^2}{6}D_3\mathbf{v}^n \\ &- \frac{\triangle t^4}{120}D_5\mathbf{v}^n - \frac{\triangle t^2}{6}F_3 - \frac{\triangle t^4}{120}F_5 + O(\triangle t^6).\end{aligned}$$

Notice that the terms inside the brackets is a fourth order approximation of $\mathbf{v}_t$. A sixth order time-stepping scheme yields

$$\frac{\mathbf{v}^{n+1}-2\mathbf{v}^{n}+\mathbf{v}^{n-1}}{\triangle\, t^2} = \tilde{B}_3\frac{\mathbf{v}^{n+1}-\mathbf{v}^{n-1}}{2\,\triangle\, t} + \tilde{D}_3\mathbf{v} + \tilde{F}_3^n, \tag{57}$$

where

$$\begin{aligned}\tilde{B}_3 &= \tilde{B}_2 + \frac{\triangle t^4}{360}\left(B_6 - 3B_2B_5 - 5B_4B_3 + 10B_2{B_3}^2\right), \\ \tilde{D}_3 &= \tilde{D}_2 + \frac{\triangle t^4}{360}\left(D_6 - 3B_2D_5 - 5B_4D_3 + 10B_2B_3D_3\right) \\ \tilde{F}_3^n &= F + \frac{\triangle t^2}{12}F_4 + \frac{\triangle t^4}{360}F_6 - \frac{\triangle t^4}{72}B_4F_3 + B_2\left(\frac{\triangle t^4}{36}B_3F_3 - \frac{\triangle t^2}{6}F_3 - \frac{\triangle t^4}{12}F_5\right)\end{aligned}$$

Using (40) and collecting terms we have

$$\begin{aligned}\tilde{B}_3 &= \tilde{B}_2 + \frac{\triangle t^4}{360}\bar{B}_3, \\ \bar{B}_3 &= 3B^5 + 3B^3D + 3BDB^2 + 3BD^2 - 2B^2DB - 4DB^3 - 4DBD + D^2B,\end{aligned}$$

$$\tilde{D}_3 = \tilde{D}_2 + \frac{\triangle t^4}{360}\bar{D}_3,$$
$$\bar{D}_3 = 3B^4D + 3BDBD - 4DB^2D - 2B^2D^2 + D^3.$$

For $B = \beta\mathbf{I}$, $\beta \leq 0$ is a constant, and we can put $\tilde{B}_3, \tilde{D}_3$ in the form (29). Now consider $\tilde{D}_3$, set $B = \beta\mathbf{I}$ and $D = -H^{-1}A$, we have

$$\tilde{D}_3 = -H^{-1}\left(H - \frac{\triangle t^2}{12}\left(A + \beta^2 H\right)\right)H^{-1}A$$
$$- H^{-1}\left(\frac{\triangle t^4}{360}\left(3\beta^4 H + 3\beta^2 H + 3\beta^2 A + AH^{-1}A\right)\right)H^{-1}A,$$

and we have

$$\tilde{A}_3 = A = \tilde{A}_3^T \geq 0.$$

For

$$\tilde{H}_3 = H\left(H - \frac{\triangle t^2}{12}\left(A + \beta^2 H\right) + \frac{\triangle t^4}{360}\left(3\beta^4 H + 3\beta^2 H + 3\beta^2 A + AH^{-1}A\right)\right)^{-1} H,$$

we have the lemma
Lemma 8 *If the condition*

$$\frac{\triangle t^2}{12}\left(\max_j |\lambda_j| + |\beta|_H^2\right) < \min_j \sigma_j, \tag{58}$$

holds, then $\tilde{H}_3$ is symmetric and positive definite, $\tilde{H}_3 = \tilde{H}_3^T > 0$.

For $\tilde{B}_3$ we have

$$\tilde{B}_3 = \tilde{H}_3^{-1}\left(\tilde{H}_3\tilde{B}_3\right) = -\tilde{H}_3^{-1}\tilde{C}_3,$$

$$\tilde{C}_3 = -\tilde{H}_3\tilde{B}_3 = -\left(\beta - \frac{\triangle t^2}{12}\beta^3 + \frac{\triangle t^4}{120}\beta^5\right)\tilde{H}_3,$$

and

$$\tilde{C}_3 + \tilde{C}_3^* = -\left(\left(\beta - \frac{\triangle t^2}{12}\beta^3 + \frac{\triangle t^4}{120}\beta^5\right) + \left(\beta - \frac{\triangle t^2}{12}\beta^3 + \frac{\triangle t^4}{120}\beta^5\right)^*\right)\tilde{H}_3.$$

Lemma 9 *Assuming $B = \beta\boldsymbol{I}$, $\beta \leq 0$ is a constant and (8) holds, then*

$$\tilde{C}_3^* + \tilde{C}_3 \geq 0.$$

The result here is:

Theorem 6 *Consider the fully discrete problem (57), assume that* $B = \beta \boldsymbol{I}$, $\beta \leq 0$, *if the conditions*

$$\frac{\triangle t^2}{12}\left(\max_j |\lambda_j| + |\beta|_H^2\right) < \min_j \sigma_j,$$

and

$$\frac{\triangle t^2}{4}\max_j |\lambda_j| < \min_j \sigma_j,$$

hold, the sixth order approximation (57) is stable and the discrete energy $\tilde{\mathcal{E}}_3^{n+1}$, *is bounded for any* $n \geq 0$.

Remark 1 *In computations however, for the sixth order case we see strict stability as long as* $C^* + C \geq 0$, *although we could not show theoretically that* $\tilde{H}_3 = \tilde{H}_3^T > 0$ *and* $\tilde{C}_3 + \tilde{C}_3^* \geq 0$. *Note that* $\tilde{B}_3$, $\tilde{D}_3$ *are 4-th order corrections of* $\tilde{B}_2$, $\tilde{D}_2$. *If* $\triangle t$ *is small enough the symmetric parts of* $\tilde{B}_3$, $\tilde{D}_3$ *satisfying assumption i) – iii) of (29) dominate. We also note that the scheme could be generalized to arbitrary order of accuracy.*

To initialize the scheme we consider the Taylor expansion (59)

$$\begin{aligned}\mathbf{v}(t+\triangle t) &= \mathbf{v}(t) + \triangle t \mathbf{v}_t(t) + \frac{\triangle t^2}{2}\left(B\mathbf{v}_t(t) + D\mathbf{v}(t) + F(t)\right)\\ &+ \sum_{k=3}^{2m}\frac{(\triangle t)^k}{k!}\left(B_k\mathbf{v}_t(t) + D_k\mathbf{v}(t) + F_k(t)\right) + O(\triangle t^{2m+1}).\end{aligned} \tag{59}$$

A high order approximation of the solution at $t_1 = \triangle t$ yields

$$\begin{aligned}\mathbf{v}(\triangle t) &= \mathbf{v}(0) + \triangle t \mathbf{v}_t(0) + \frac{\triangle t^2}{2}\left(B\mathbf{v}_t(0) + D\mathbf{v}(0) + F(0)\right)\\ &+ \sum_{k=3}^{2m}\frac{(\triangle t)^k}{k!}\left(B_k\mathbf{v}_t(0) + D_k\mathbf{v}(0) + F_k(0)\right) + O(\triangle t^{2m+1}).\end{aligned} \tag{60}$$

References

[1] K. Duru, G. Kreiss, *A Well-posed and discretely stable perfectly matched layer for elastic wave equations in second order formulation*, Tech Rep, Div Sc. Comp., Dept. of Infor Tech., Uppsala University, ISSN 1404-3203, 2010-04, 2010.

[2] B. Sjögreen, N. A. Petersson, *Perfectly matched layer for Maxwell's equation in second order formulation*, J Comp Phys, 209, p19-46, 2005.

[3] M. J. Grote, T. Mitkova, *Explicit local time-stepping methods For Maxwell's Equations*, Dept. of Maths University of Basel, Preprint No. 2009-02, 2009.

[4] K. Mattsson , J. Nordström, *High order finite difference methods for wave propagation in discontinuous media* , J Comp Phys, 220, p249–269, 2006.

[5] M. Svärd , J. Nordström, *On the order of accuracy for difference approximations of initial-boundary value problems*, J Comp Phys, 218, p333–352, 2006.

[6] K. Mattsson, F. Ham, G. Iaccarinoa, *Stable and accurate wave-propagation in discontinuous media* , J Comp Phys, 227, p8753–8767, 2008.

[7] K. Mattsson, F. Ham, G. Iaccarinoa, *Stable boundary treatment for the wave equation in second-order form*, J Sci Comput, 41, p336–383, 2009.

[8] N. A. Petersson, B. Sjögreen, *An energy absorbing far-field boundary condition for the ElasticWave Equation*, Commun. Comput. Phys., 6, p 483-508, 2009.

[9] Ken Mattsson and Jan Nordström, *Summation by Parts Operators for Finite Difference Approximations of Second Derivatives*, J. Compt. Phys., 199 (2): 503-540, September 2004.

[10] J. Diaz, M. J. Grote, *Energy conserving explicit local time-stepping for second-order wave equations*, SIAM J. Sci. Comput., 31 1985–2014, 2009.

[11] J. C.Gilbert, P. Joly, *Higher order time stepping for second order hyperbolic problems and optimal CFL conditions,* Num. Analys and Sci Comp for PDEs and their Challenging Applicat, vol. 16, pp. 67–93, Springer, 2008.

[12] H–O. Kreiss, N. A. Petersson, J. Yström, *Difference approximations for second order wave equation*, SIAM J. Num. Anal, 40, p 1940–1967, 2002.

[13] M. H. Carpenter, D. Gottlieb, S. Abarbanel, and W. Don, *The theoretical accuracy of Runge-Kutta time discretizations for the initial boundary value problem: A study of the boundary error* , SIAM J. SCi. Compt., vol. 16 No 6 pp. 1241–1252, 1995.

[14] M. Johansson, *Loss of high order spatial accuracy due to boundary error caused by Runge-Kutta time integration*, Tech Rep, Div Sc. Comp., Dept. of Infor. Tech., Uppsala University, 2000-013, 2000.

[15] O. Axelsson, *Iterative solution methods*, Cambridge University Press 1994.